Supporting Information

Chemical Control of Peptide Material Phase Transitions

Junjun Tan†[a], Li Zhang†[a], Ming-Chien Hsieh[ab], Jay T. Goodwin[a], Martha A. Grover[b] and David G. Lynn*[a]

[a]Departments of Biology and Chemistry, Emory University, Atlanta, GA 30322

[b] School of Chemical and Biomolecular Engineering, Georgia Institute of Technology, Atlanta, GA 30332

† These authors contributed equally

*: To whom correspondence may address: David G. Lynn, dlynn2@emory.edu

Scheme S1. Synthesis of *TTF*-CHO and *TF*-CHO monomer. The synthetic route to *TTF*-CHO is summarized below where Boc-protected phenylalanine is first converted to the Weinreb amide. After deprotecting the Boc protecting group, EDC coupling is used to couple an Fmoc-protected threonine. The *TF*-Weinreb amide is reduced to *TF*-CHO via LAH reduction and protected as the dimethyl acetal 6 *(TF-acetal)*. Another molecule of Fmoc-Thr is coupled to the N-terminus, and the final product 8 (*TTF-acetal*) is generated by deprotection of Fmoc and purification by HPLC. Once the acetal protection is removed, the *TF-CHO* and *TTF-CHO* are activated to give rise to dynamic chemical networks (DCNs) under suitable conditions.

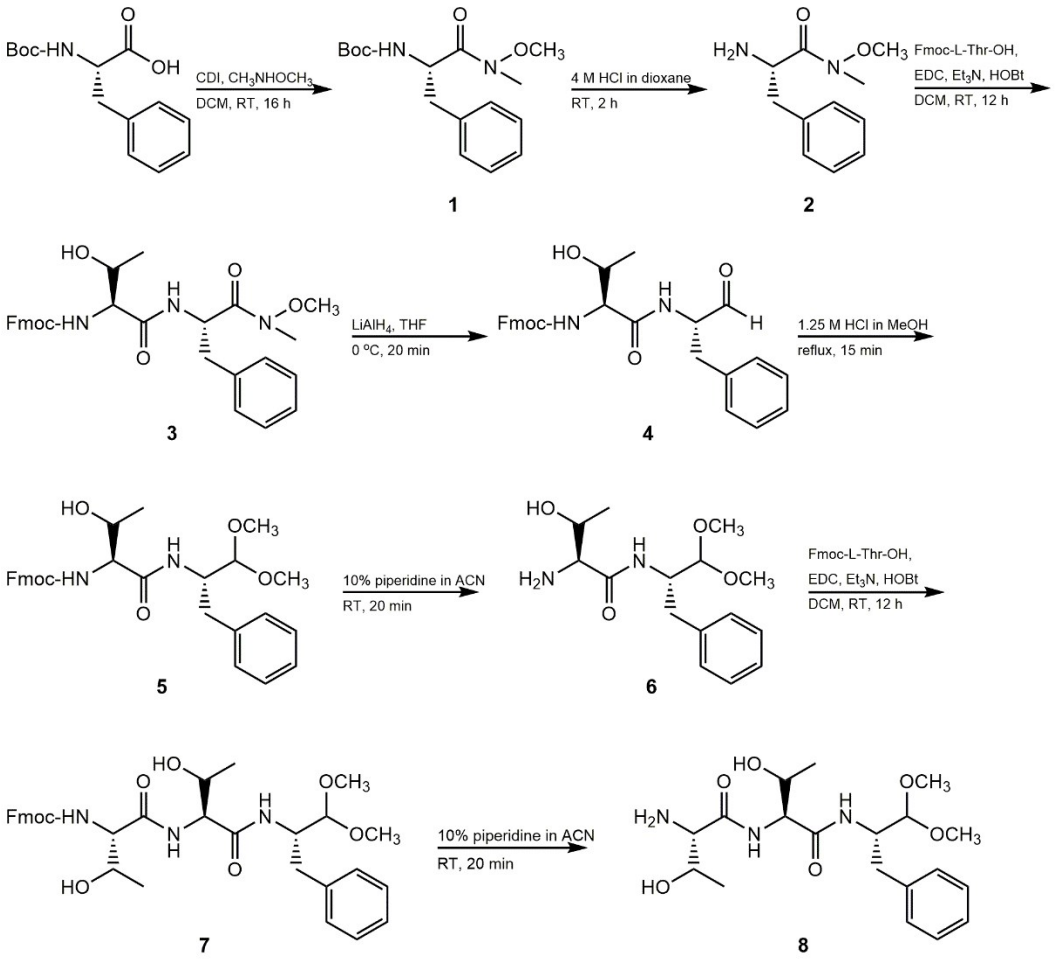

1. Boc-Phe-Weinreb amide (**1**):

To a solution of N-Boc-L-Phe 10.61 g (40 mmol) in DCM was added 7.13 g 1,1-carbonlydiimidazole (1.1 eq). After stirring for 1 h, 4.29 g (1.1 eq) N,O-dimethylhydroxylamine hydrochloride was added and the solution stirred overnight under N_2 at room temperature. The solvent was removed *in vacuo* and the residue was dissolved in EtOAc, washed with 1 M HCl (aq) three times, saturated $NaHCO_3$ twice and brine twice. The organic layer was dried with $MgSO_4$ and solvent was removed *in vacuo* to yield **1** in 92%. ^1H NMR (600 MHz, cdcl$_3$) δ 7.44 – 7.11 (m, 5H), 5.15 (d, J = 7.9 Hz, 1H), 4.94 (d, J = 6.6 Hz, 1H), 3.65 (s, 3H), 3.16 (s, 3H), 3.05 (dd, J = 13.3, 5.7 Hz, 1H), 2.85 (dt, J = 64.4, 32.2 Hz,

1H), 1.38 (s, 9H). HRMS for $C_{16}H_{25}N_2O_4$ (M+H): calcd: 309.18143, found: 309.18130.

2. Phe-Weinreb amide (**2**):

Compound **1** was dissolved in 4 M HCl in dioxane and stirred for 2 h at room temperature, then dried *in vacuo* to yield **2**, 100%. ^{1}H NMR (600 MHz, cdcl$_3$) δ 8.56 (s, br), 7.34 – 7.15 (m, 5H), 4.73 (d, *J* = 5.1 Hz, 1H), 3.64 (s, 1H), 3.35 (tt, *J* = 20.6, 6.8 Hz, 1H), 3.10 (s, 3H). HRMS for $C_{11}H_{17}N_2O_2$ (M+H): calcd: 209.12900; found: 209.12824

3. Fmoc-Thr-Phe-Weinreb amide (**3**):

One g of **2** (4.09 mmol) was dissolved in DCM. 1.2 mL (2.1 eq) of Et_3N was added, followed by 0.8626 g (1.1 eq) of N-(3-dimethylaminopropyl)-N′-ethylcarbodiimide hydrochloride (EDC). The solution turned slurry. 1.534 g (1.1 eq) of Fmoc-L-Thr-OH and 0.687 g (1.1 eq) of HOBt were subsequently added and reaction mixture was stirred for 6 h under RT. The reaction was washed with 1 M HCl (aq) twice, saturated $NaHCO_3$ solution twice then brine once. The organic layer was combined, dried with $MgSO_4$ and removed the solvent under reduced pressure to give **3**. Yield: 80%. ^{1}H NMR (600 MHz, cdcl$_3$) δ 7.77 (d, *J* = 7.5 Hz, 2H), 7.59 (d, *J* = 7.3 Hz, 2H), 7.44 – 7.08 (m, 9H), 6.82 (d, *J* = 7.6 Hz, 1H), 5.56 (d, *J* = 7.9 Hz, 1H), 5.18 (m, 1H), 4.47 (dd, *J* = 10.6, 7.2 Hz, 1H), 4.36 – 4.29 (m, 1H), 4.25 (s, 1H), 4.21 (t, *J* = 7.0 Hz, 1H), 4.12 (dd, *J* = 11.3, 5.9 Hz, 1H), 3.76 (s, 3H), 3.21 (s, 3H), 3.14 (dd, *J* = 13.8, 5.0 Hz, 1H), 3.05 (s, 1H), 2.91 – 2.77 (m, 1H), 1.11 (t, *J* = 9.2 Hz, 3H). HRMS for $C_{30}H_{34}N_3O_6$ (M+H): calcd: 532.24476; found: 532.24424.

4. Fmoc-Thr-Phe-aldehyde (**4**):

Compound **3** (2.173 g, 4.08 mmol) was dissolved in THF under N_2. The solution was cooled down to -78 ^{o}C before 1.4 eq of lithium aluminum hydride (1.0 M in THF, 5.7 mL) was added dropwise via syringe. The reaction mixture was warmed to 0 ^{o}C and stirred for 30 min before being cooled to -78 ^{o}C again and 57 mL of 1 M $KHSO_4$ (aq) was added to quench the reaction. The THF was removed *in vacuo* and the residue dissolved in EtOAc, washed with saturated $NaHCO_3$ and brine. The organic layer was dried with $MgSO_4$ before concentration to yield aldehyde **4** in 91% yield. ^{1}H NMR (600 MHz, cdcl$_3$) δ 9.63 (s, 1H), 7.78 (d, *J* = 7.4 Hz, 2H), 7.60 (m, 2H), 7.39-7.10 (m, 9H), 5.61 (d, *J* = 8.0 Hz, 1H), 4.73 (dd, *J* = 13.8, 7.0 Hz, 1H), 4.48 (dd, *J* = 10.6, 6.9 Hz, 1H), 4.39 – 4.28 (m, 1H), 4.12 (dd, *J* = 14.2, 7.1 Hz, 1H), 3.12 (ddd, *J* = 21.5, 14.2, 6.8 Hz, 2H), 1.14 (t, *J* = 11.2 Hz, 3H). HRMS for $C_{28}H_{29}N_2O_5$ (M+H): calcd: 473.20765, found: 473.20789

5. Fmoc-Thr-Phe-acetal (**5**):

Compound **4** (1.234 g) was dissolved in 20 mL 1.25 M HCl in MeOH, refluxed at 75 ^{o}C for 15 min, cooled to RT and quenched with saturated $NaHCO_3$. The MeOH was removed under reduced pressure and the residue dissolved EtOAc, washed with sat $NaHCO_3$ water, dried *in vacuo*, and purified by silica gel column (Hexanes: EtOAc = 1:3) to give **5** in 94% yield. ^{1}H NMR (600 MHz, cdcl$_3$) δ 7.78 (d, *J* = 7.4 Hz, 2H), 7.60 (d, *J* = 7.1 Hz, 2H), 7.42 -7.15 (m, 9H), 6.43 (d, *J* = 8.9 Hz, 1H), 5.53 (d, *J* = 8.2 Hz, 1H), 4.50 (dd, *J* = 10.4, 7.0 Hz, 1H), 4.43 (tdd, *J* = 9.2, 5.7, 3.3 Hz, 1H), 4.34 (dd, *J* = 10.5, 7.1 Hz, 1H), 4.27 – 4.16 (m, 2H), 4.03 (d, *J* = 8.2 Hz, 1H), 3.44 (s, 3H), 3.39 (s, 3H), 2.95 (dd, *J* = 14.0, 5.9 Hz, 1H), 2.86 (s, 1H), 2.71

(dd, *J* = 13.9, 9.0 Hz, 1H), 1.11 (d, *J* = 6.4 Hz, 3H). HRMS for $C_{30}H_{35}N_2O_6$ (M+H): calcd: 519.24951, found: 519.24697.

6. Thr-Phe-acetal (***TF-acetal***) (**6**):

1.104 g **5** was suspended in 10 mL acetonitrile, 2 mL piperidine was added and stirred for 20 min at room temperature before the solvent was removed *in vacuo* to yield **6**, 70%. ^{1}H NMR (600 MHz, cdcl$_3$) δ 7.45 (d, *J* = 9.7 Hz, 2H), 7.37 – 7.21 (m, 2H), 7.19 (dd, *J* = 10.4, 4.2 Hz, 3H), 4.48 – 4.39 (m, 1H), 4.18 (t, *J* = 41.9 Hz, 1H), 4.07 (dq, *J* = 9.6, 3.2 Hz, 1H), 3.46 (s, 3H), 3.42 (s, 3H), 3.14 (d, *J* = 3.1 Hz, 1H), 3.04 – 2.93 (m, 1H), 2.72 (dd, *J* = 14.0, 9.7 Hz, 1H), 1.01 (d, *J* = 6.5 Hz, 3H). HRMS for $C_{15}H_{25}N_2O_4$ (M+H): calcd: 297.18143, found: 297.18097.

7. Fmoc-Thr-Thr-Phe-acetal (**7**)

Same procedure as step 3. After removing the solvent, the product was purified by flash column with DCM: MeOH = 50:1 to 20:1. Yield: 74%. ^{1}H NMR (600 MHz, cdcl$_3$) δ 7.75 (d, J = 7.5 Hz, 2H), 7.57 (d, J = 7.4 Hz, 2H), 7.39-7.01 (m, 9H), 6.63 (d, J = 9.0 Hz, 1H), 5.72 (d, J = 7.7 Hz, 1H), 4.53 – 4.32 (m, 3H), 4.33 – 4.15 (m, 5H), 3.42 (s, 3H), 3.36 (s, 3H), 2.92 (dd, J = 14.0, 5.7 Hz, 1H), 2.74 (dd, J = 13.9, 8.8 Hz, 1H), 1.14 (d, J = 6.3 Hz, 3H), 1.06 (d, J = 6.4 Hz, 3H). HRMS for $C_{34}H_{42}N_3O_8$ (M+H): calcd: 620.29719, found: 620.29749.

8. Thr-Thr-Phe-acetal (***TTF-acetal***) (**8**):

Same procedure as step 6. Purified by HPLC to give final product **8**. Yield: 78%. ^{1}H NMR (400 MHz, DMSO) δ 8.00 (d, J = 8.5 Hz, 1H), 7.79 (d, J = 8.9 Hz, 1H), 7.31 – 7.13 (m, 4H), 4.81 (d, J = 4.8 Hz, 1H), 4.76 (d, J = 4.0 Hz, 1H), 4.24 (d, J = 4.5 Hz, 1H), 4.17 (dd, J = 8.0, 4.0 Hz, 1H), 4.10 (ddd, J = 13.2, 9.1, 4.1 Hz, 1H), 4.00 – 3.92 (m, 1H), 3.89 (dd, J = 11.0, 4.9 Hz, 1H), 3.38 (s, 3H), 3.35 (s, 3H), 3.08 (d, J = 4.2 Hz, 1H), 2.88 (dd, J = 14.1, 3.5 Hz, 1H), 2.67 (dd, J = 14.1, 9.8 Hz, 1H), 1.07 (d, J = 6.4 Hz, 3H), 0.97 (t, J = 14.1 Hz, 3H). HRMS for $C_{19}H_{32}N_3O_6$ (M+H): calcd: 398.22911, found: 398.22925

Scheme S2. *TF*-CHO reversibly cyclizes and is susceptible to irreversible oxidation to the pyrazine.

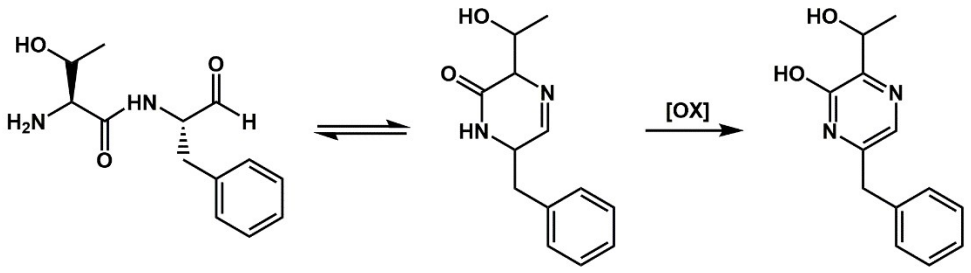

Scheme S3. ODEs for concentration change for *TTF*-CHO monomer (*M*), *TTF*-CHO cyclic dimer (D_c), TTF*ox*TTFTTF trimer (*T*), H-TTFTTF-NH_2 peptide (D_p), assembled trimer (*A*) and assembly number (*P*). k_1 = dimer formation constant. k_2 = dimer breakage constant. k_3 = trimer formation constant. k_4 = trimer breakage constant. k_5 = assembly nucleation constant. k_6 = assembly growth constant. k_7 = assembly breakage constant. k_8 = templating constant. n_c = assembly critical size, in this case 2[1].

$$\frac{dM}{dt} = -2k_1M^2 + 2k_2D_c - k_3MD_p + k_4T - 2k_8MPT$$

$$\frac{dD}{dt} = k_1M^2 - k_2D_c$$

$$\frac{dT}{dt} = k_3MD_p - k_4T - 2\left(k_6T - k_7\right)P - n_ck_5T^{n_c}$$

$$\frac{dD_p}{dt} = -k_3MD_p + k_4T - 2k_8MPT$$

$$\frac{dA}{dt} = 2\left(k_6T - k_7\right)P + n_ck5T^{nc} + 2k_8MPT$$

$$\frac{dP}{dt} = k_7\left(A - P\left(2n_c - 1\right)\right) + k_5T^{n_c}$$

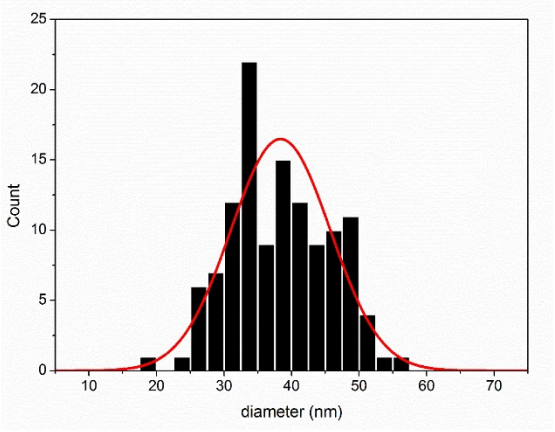

Figure S1. Histogram defining a Gaussian distribution of $(TTF)_3$ nanotube diameters. Nanotube width is measured with ImageJ counting at least 120 tubes, and converting into diameters by setting 2 × width = the tube circumference and solving for the diameter. The Gaussian fits give an average diameter of 38.4 ± 7.4 nm.

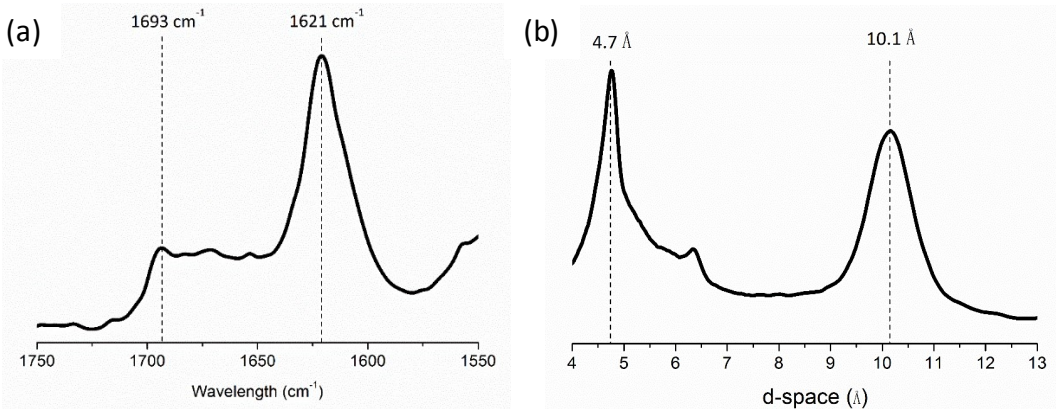

Figure S2. FT-IR and X-ray powder diffraction analyses of the $(TTF)_3$ nanotubes. (a) FT-IR amide I band at 1621 cm^{-1} with a weak transition at 1693 cm^{-1} is consistent with anti-parallel β-sheet orientation. (b) X-ray powder diffraction with d-spacing at 4.7 Å and 10.1 Å corresponding to H-bonded strand spacing and sheet lamination repeat distances in cross-β assemblies.

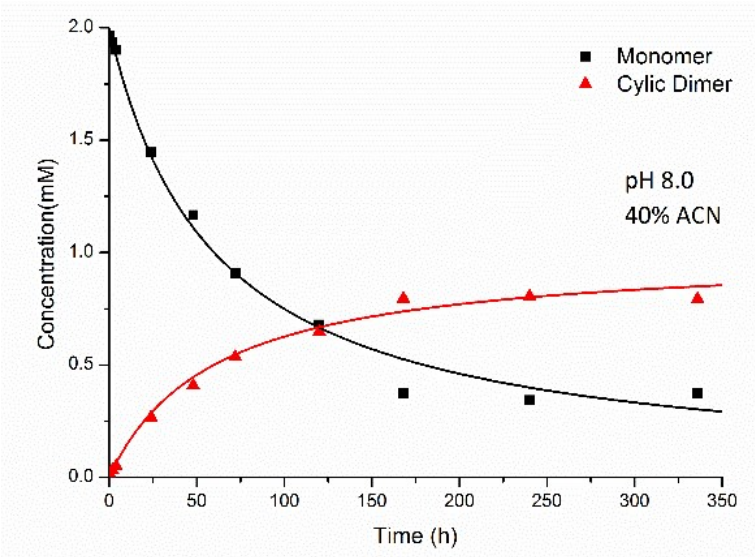

Figure S3. *TTF*-CHO generates a DCN with cyclic dimer as dominant species.

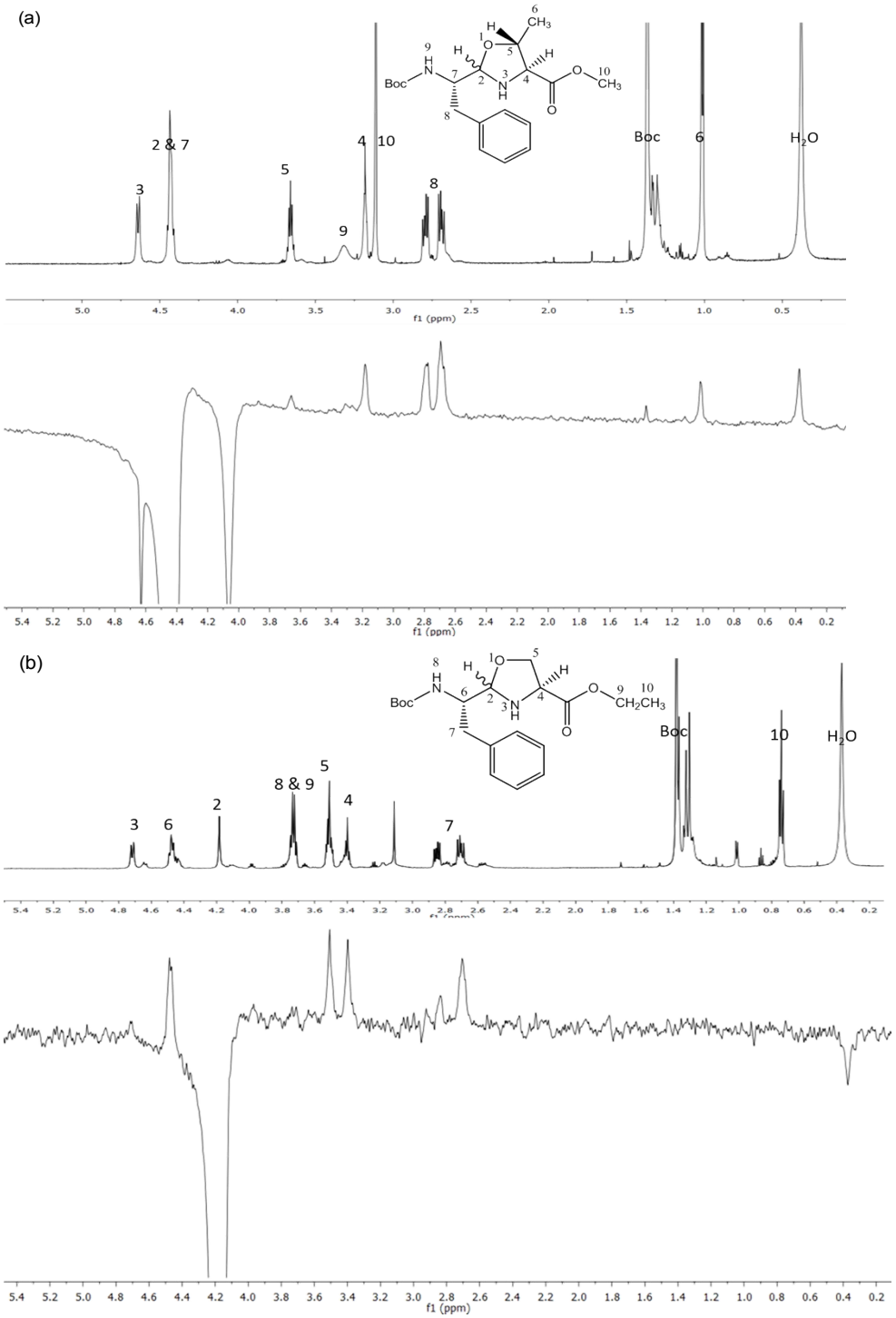

Figure S4. 1D-NMR NOE difference spectra of the N,O-acetal (a) F*ox*T and (b) F*ox*S peptide prepared by condensation of N-Boc-L-Phe-CHO with either L-Thr or L-Ser methyl ester in refluxing benzene. In benzene-d6, irradiation of the acetal H2 resonance of F*ox*T gives positive enhancement of H4 but not H5, indicating H2 and H4 are on the same face of the ring, supporting the acetal (R, S)-*cis* configuration. Overlap of H2 and H7 resonance results in H8 enhancement as well. Similarly, for the F*ox*S product, irradiation of acetal H2 resonance gives positive enhancement of H4, also positions H2 and H4 on the same side of the ring.

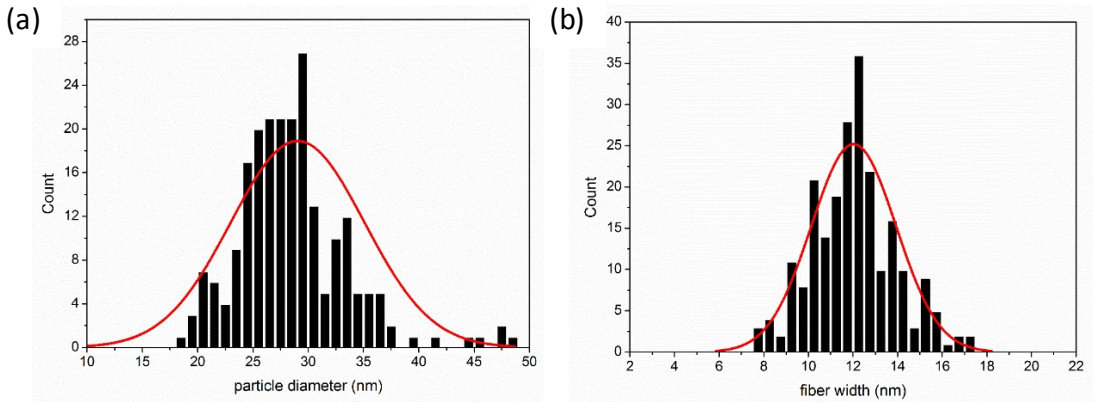

Figure S5. Histograms and Gaussian distribution of particle and fiber sizes. (a) Particles at 24h, with widths of 29.0 ± 3.0 nm. (b) Mature fibers at 10 days with widths of 12.03 ± 1.90 nm.

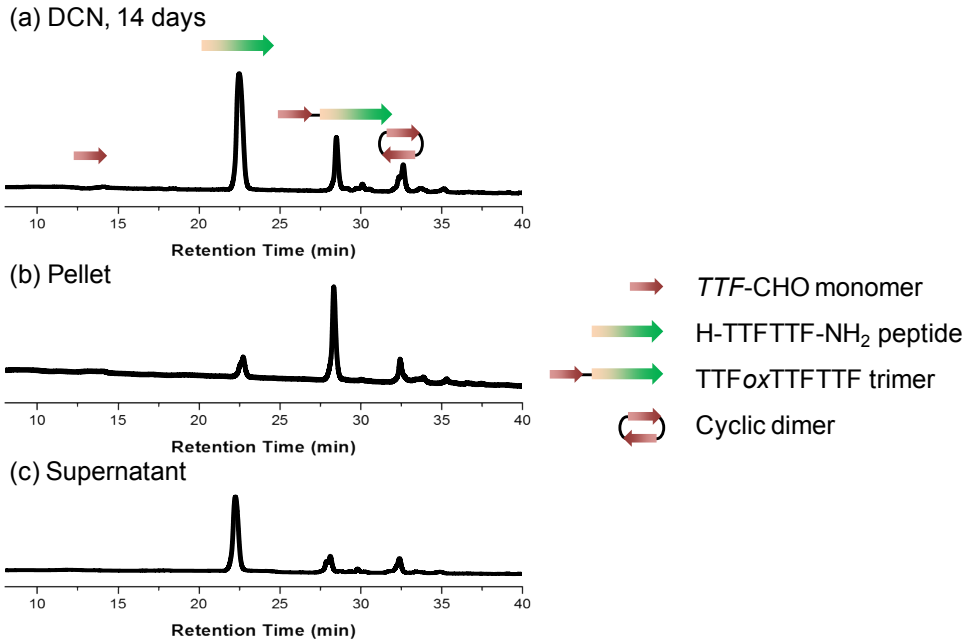

Figure S6. HPLC analyses of *TTF*-CHO + H-TTFTTF-NH_2 network. (a) Analysis of the entire network on Day 14, and after centrifuging at 16,000 × g for 30 min and re-injection of (b) the pellet and (c) the supernatant.

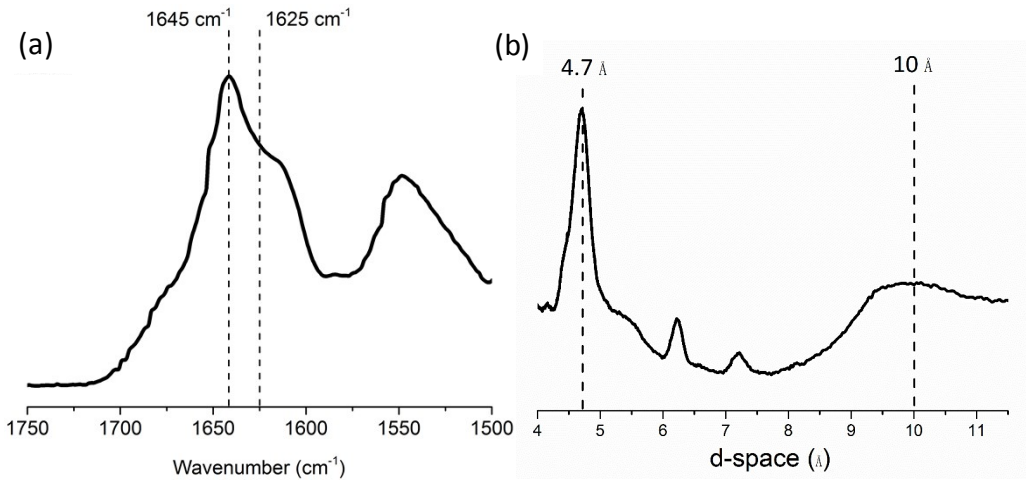

Figure S7. Characterization of the TTF*ox*TTFTTF fibers by FT-IR and XRD. (A) the FT-IR contains amide I transitions at 1645 cm^{-1} with a shoulder at ~1625 cm^{-1} (B) XRD contains a sharp reflection at a d-spacing of 4.7 Å, consistent with strand H-bonding distances, and a broad 10 Å d-spacing consistent with sheet lamination.

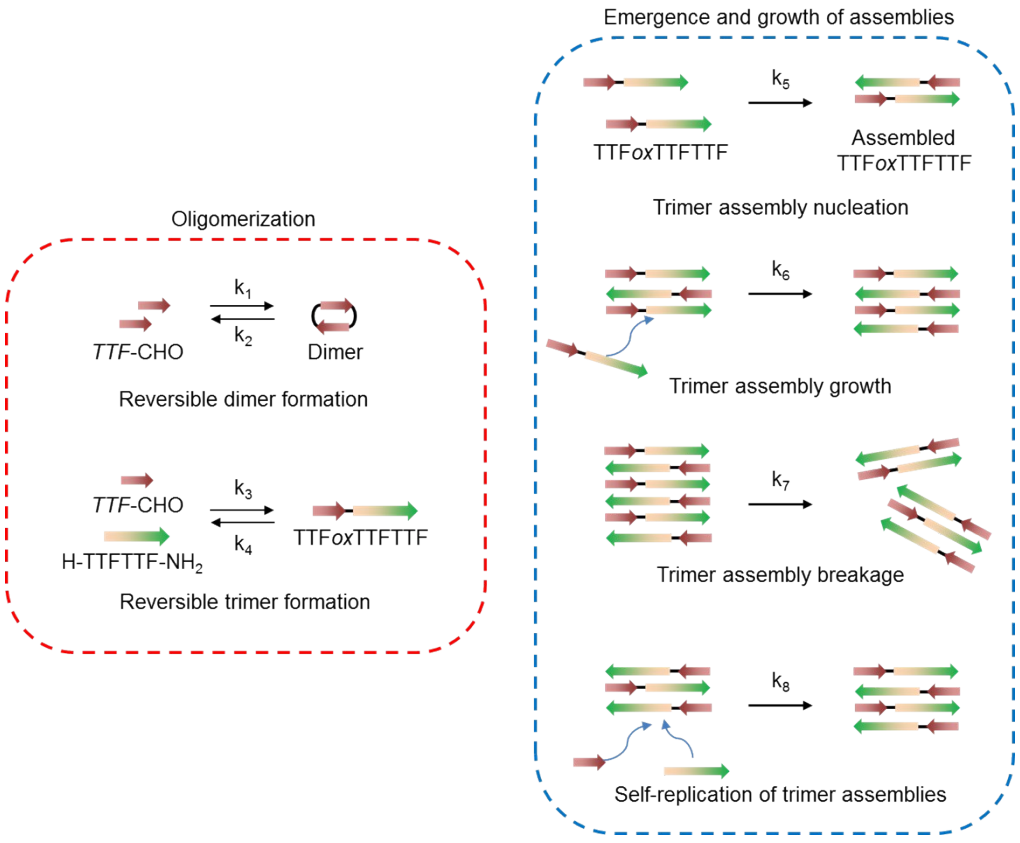

Figure S8. **Reaction scheme for the *TTF*-CHO + H-TTFTTF-NH_2 network.**

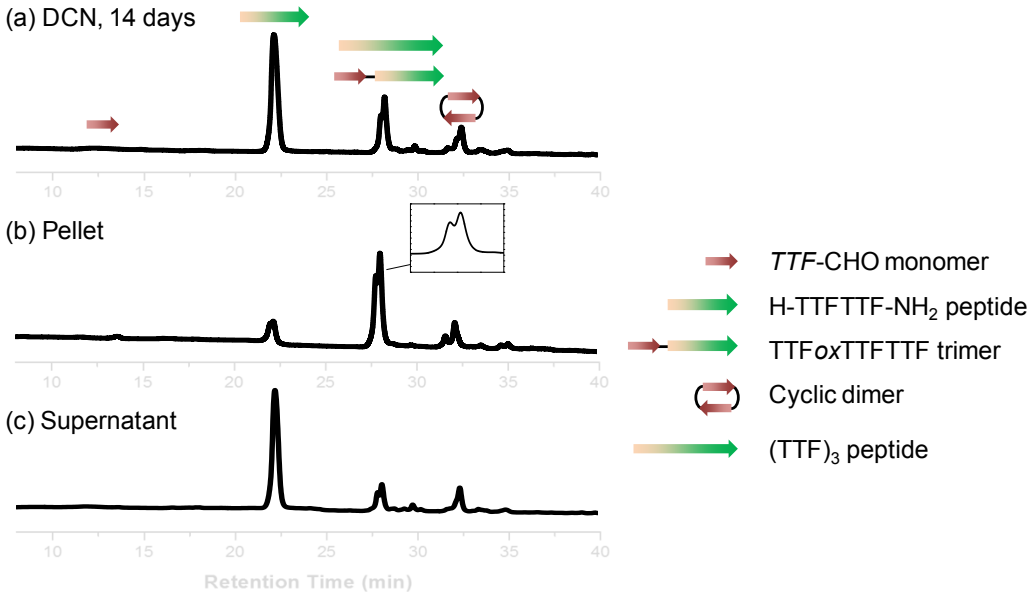

Figure S9. HPLC analysis of the $(TTF)_3$ nanotube seeded *TTF*-CHO/H-TTFTTF-NH_2 network. Traces of (a) mature DCN network, (b) re-injection of pellet enriched by centrifugation at 16000×g indicating the elution of TTF*ox*TTFTTF and $(TTF)_3$, and (c) analysis of the supernatant.

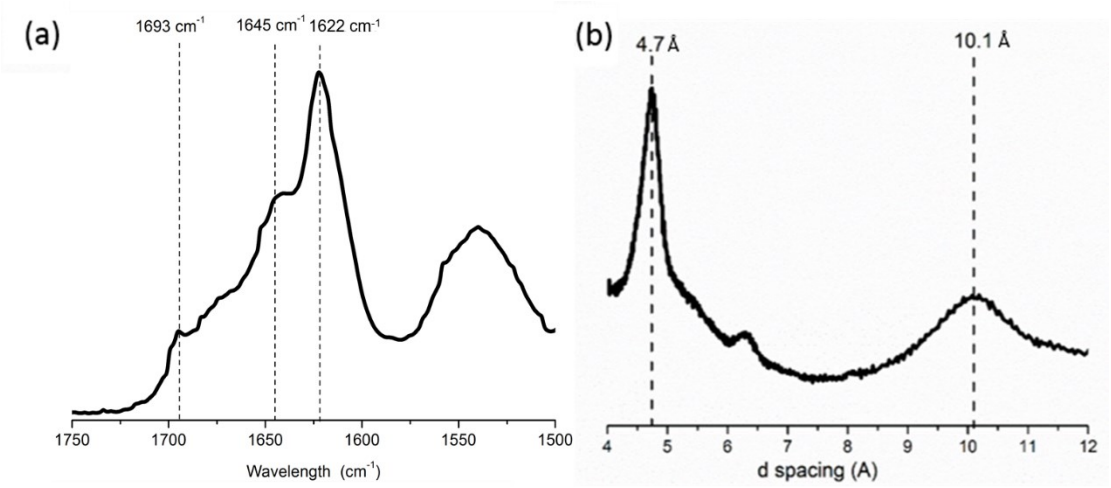

Figure S10. Spectral analyses of the $(TTF)_3$ nanotube-templated *TTF*-CHO network. (A) FT-IR contains transitions at 1622 cm^{-1} amide I transition with a 1693 cm^{-1} band, consistent with anti-parallel β-sheets. (B) XRD assigned d-spacing of 4.7 Å for the H-bonding strand repeats and 10.1 Å for the sheet lamination distance of cross-β assemblies.

Table S1. Mass spectral identification of species generated in *TTF*-CHO network

species	m/z found	m/z calculated
TTF-CHO	352.1866	352.1872 ($M+H^+$: $C_{17}H_{26}N_3O_5$)
Cyclic dimer	667.3446	667.3455 ($M+H^+$: $C_{34}H_{47}N_6O_8$)
Cyclic trimer	1000.5136	1000.5144 ($M+H^+$: $C_{51}H_{70}N_9O_{12}$)
Cyclic tetramer	1371.6511	1371.6391($M+K^+$: $C_{68}H_{92}N_{12}O_{16}K$)

Table S2. The reactions and the corresponding equations for the *TTF*-CHO + H-TTFTTF-NH_2 network. M is *TTF*-CHO monomer concentration, D_c is the dimer concentration, k_1 the formation constant, k_2 the breakage constant, D_p the H-TTFTTF-NH_2 peptide concentration, T the TTF*ox*TTFTTF trimer concentration, k_3 the formation constant, k_4 the breakage constant, n_c the critical nucleus size, k_5 the nucleation constant, k_6 the assembly growth constant, k_7 the assembly breakage constant, P the assembly number concentration, A the concentration of assembled trimer, and k_8 is the templating constant.

Reaction	Equation	Reference
cyclic dimer formation	k_1M^2	
cyclic dimer breakage	k_2D_c	
TTF*ox*TTFTTF formation	k_3MD_p	
TTF*ox*TTFTTF breakage	k_4T	
TTF*ox*TTFTTF self-assembly	$n_ck_5T^{n_c}+2\left(k_6T-k_7\right)P$	[1]
change of assembly number	$k_5T^{n_c}+k_7\left(A-P\left(2n_c-1\right)\right)$	[1]
self-templating	$2k_8MTP$	

Table S3. Rate constants for the *TTF*-CHO/H-TTFTTF-NH_2 network fit to Scheme S3 and in Figure 3.

Parameter	Value
k_1 ($mM^{-1}sec^{-1}$)	6.77×10^{-07}
k_2 (sec^{-1})	5.71×10^{-10}
k_3 ($mM^{-1}sec^{-1}$)	7.63×10^{-06}
k_4 (sec-1)	6.08×10^{-04}
k_5 ($mM^{-1}sec^{-1}$)	4.68×10^{-04}
k_6 ($mM^{-1}sec^{-1}$)	1.70×10^{-08}
k_7 (sec^{-1})	2.54×10^{-06}
k_8 ($mM^{-2}sec^{-1}$)	2.81×10^{-06}

Kinetic analyses and model discrimination

The growth of trimer appears as a simple second-order reaction, and the assemblies reach equilibrium without consuming all the *TTF*-CHO monomer and H-TTFTTF-NH_2, suggesting that a simpler mechanism without the terms of self- assembly may be built. Here the corrected Akaike information criterion[2] and the Akaike weight[3] are used to test the importance of the self-assembly and templating reactions. Totally five candidates are tested (Table S4). The first three candidates in Table S4 have the same SSE, resulting from a zero-assembly nucleation constant (k_5) for all, because of either restriction or parameter optimization. This is consistent with the reversible nature of trimer self-assembly. Without the assembly breakage constant (k_7), the models do not fit the data well with solely irreversible assembly growth. Among five candidates, the most complicated model, the full one with no restriction, has the highest Akaike weight. More information is preserved when the most complicated model is used suggesting that even though not obvious in the chemical steps, the assembly process is critical to the observed kinetics.

Table S4. AIC_c analysis of Scheme S1 fits to the *TTF*-CHO network concentrations with single- and two-stage models, where N_d is the number of data points, and N_p is the number of parameters.

Restriction	N_d	SSE	N_p	AIC_c	Akaike weight (%)
$k_5 = k_6 = k_7 = k_8 = 0$	57	0.0472	4	-395.7	19.5
$k_6 = k_7 = k_8 = 0$	57	0.0472	5	-393.3	5.8
$k_7 = k_8 = 0$	57	0.0472	6	-390.8	1.7
$k_8 = 0$	57	0.0447	7	-391.3	2.1
No restriction	57	0.0377	8	-398.3	70.9

Table S5. Mass spectrometry identification of assembly species in seeded DCN.

species	m/z found	m/z calcd
TTF*ox*TTFTTF	1049.5330	1049.5308 ($M+H^+$: $C_{51}H_{73}N_{10}O_{14}$)
$(TTF)_3$ peptide	1166.6481	1166.6461 ($M+Et_3N+H^+$: $C_{57}H_{88}N_{11}O_{15}$)

References

1. T. P. J. Knowles, C. A. Waudby, G. L. Devlin, S. I. A. Cohen, A. Aguzzi, M. Vendruscolo, E. M. Terentjev, M. E. Welland and C. M. Dobson, *Science*, 2009, **326**, 1533-1537.
2. C. M. Hurvich and C.-L. Tsai, *Biometrika*, 1989, **76**, 297-307.
3. E.-J. Wagenmakers and S. Farrell, *Psychonomic Bulletin & Review*, 2004, **11**, 192-196.